Available online at www.sciencedirect.com
SciVerse ScienceDirect
www.elsevier.com/locate/brainres
Brain Research

Research Report

Vasopressin-induced intracellular Ca^{2+} concentration responses in non-neuronal cells of the rat dorsal root ganglion

Taiki Moriya[a], Tomohiko Kayano[a], Naoki Kitamura[a], Yoshinao Z. Hosaka[b], Atsushi Asano[c], Oksana Forostyak[d], Alexei Verkhratsky[d,e], Cedric Viero[f], Govindan Dayanithi[d,g], Emil C. Toescu[h], Izumi Shibuya[a,]*

[a]*Department of Veterinary Physiology, Faculty of Agriculture, Tottori University, Tottori 680-8553, Japan*
[b]*Department of Veterinary Anatomy, Faculty of Agriculture, Tottori University, Tottori 680-8553, Japan*
[c]*Department of Veterinary Biochemistry, Faculty of Agriculture, Tottori University, Tottori 680-8553, Japan*
[d]*Department of Molecular Signalling, Institute of Experimental Medicine, Academy of Sciences of the Czech Republic, Prague 14220, Czech Republic*
[e]*Faculty of Life Sciences, The University of Manchester, Oxford Road, Manchester, M13 9PT, UK*
[f]*Department of Cardiology, Wales Heart Research Institute, School of Medicine, Cardiff University, Cardiff, CF14 4XN, UK*
[g]*Institut National de la Santé et da la Recherche Médicale, Unité de recherche U710, Université Montpellier 2, Montpellier 34095, France*
[h]*Neuronal Network Group, School of Clinical and Experimental Medicine, College of Medical and Dental Sciences, The University of Birmingham, Birmingham, B15 2TT, UK*

ARTICLE INFO

Article history:
Accepted 15 August 2012
Available online 6 September 2012

Key words:
Neuropeptides
Peripheral nervous system
Glia
Ca^{2+} signalling
Ca^{2+} stores
Vasopressin receptors

ABSTRACT

Arginine-vasopressin (AVP) is a nonapeptide of hypothalamic origin that has been shown to exert many important cognitive and physiological functions in neurons and terminals of both the central and peripheral nervous system (CNS and PNS). Here we report for the first time that AVP induced an increase in intracellular Ca^{2+} concentration ($[Ca^{2+}]_i$) in non-neuronal cells isolated from the rat dorsal root ganglion (DRG) and cultured in vitro. The ratiometric $[Ca^{2+}]_i$ measurements showed that AVP evoked $[Ca^{2+}]_i$ responses in the non-neuronal cells and these concentration-dependent (100 pM to 1 μM) responses increased with days in vitro in culture, reaching a maximum amplitude after 4–5 day. Immunostaining by anti-S-100 antibody revealed that more than 70% of S-100 positive cells were AVP-responsive, indicating that glial cells responded to AVP and increased their $[Ca^{2+}]_i$. The responses were inhibited by depletion of the intracellular Ca^{2+} stores or in the presence of inhibitors of phospholipase C, indicating a metabotropic response involving inositol trisphosphate, and were mediated by the V_1 subclass of AVP receptors, as evidenced by the use of the specific blockers for V_1 and OT receptors, $(d(CH_2)^1_5,Tyr(Me)^2,Arg^8)$-Vasopressin and $(d(CH_2)^1_5,Tyr(Me)^2,Thr^4,Orn^8,des\text{-}Gly\text{-}NH^9_2)$-Vasotocin, respectively. V_{1a} but not V_{1b} receptor mRNA was expressed sustainably through the culture period in cultured DRG cells. These results suggest that AVP modulates the activity of DRG glial cells via activation of V_{1a} receptor.

*Correspondence to: 4-101, Koyama-cho Minami, Tottori 680-8553, Japan. Fax: +81 857 31 5425.
E-mail address: shibuya@muses.tottori-u.ac.jp (I. Shibuya).

0006-8993/$ - see front matter © 2012 Elsevier B.V. All rights reserved.
http://dx.doi.org/10.1016/j.brainres.2012.08.028

1. Introduction

The effects of the nonapeptide arginine-vasopressin (AVP) on the central nervous system (CNS) where they originate from are well established and extensively documented. They range from control of water homeostasis to stress (Volpi et al., 2004), anxiety (Bielsky et al., 2004) and social behavioral modulations (Tobin et al., 2010). AVP is synthesized in and secreted by the magnocellular neurosecretory neurons of the hypothalamo-neurohypophysial system. The action of AVP is mediated through a specific subtype of 7 transmembrane domains G-protein coupled receptors. The AVP receptors are represented by 3 distinct subtypes classified as V_{1a}, V_{1b} and V_2 receptors (Manning et al., 2008). The AVP system is present and/or active in peripheral organs such as heart (Dayanithi et al., 2008), smooth muscles (Karashima, 1981; Li et al., 2001; Van Putten et al., 1994) and also in the peripheral nervous system (PNS) (Bone et al., 1984). In respect to the latter case, the actual physiological role that AVP could play is still under consideration.

Dorsal root ganglia (DRG) contain the cell bodies of pseudo-unipolar neurons conveying and integrating somatic sensory inputs (pain, temperature, mechanosensation) from the periphery to the spinal cord. According to somata's diameters, one can distinguish 3 types of neurons: large, medium and small, corresponding to different conductivities and sensory modalities (Scroggs and Fox, 1992). Obviously, the classification of DRG neurons is much more complex and is also based on the action potential configuration, the level of myelination and the expression of important molecular markers such as ion channels (Lechner et al., 2009).

DRG neurons are surrounded by both satellite glial cells (Hanani, 2005) and myelinating Schwann cells. Both types of the DRG glial cells are derived from neural crest (Jessen and Mirsky, 2005; Le Douarin et al., 1991), and express S-100 protein (Vega et al., 1991) but have several differences in their functions and localization.

The satellite glial cells surround completely around the cell bodies of DRG neurons, and the distance between the two types of cells is about 20 nm (Pannese, 1981). Little is known about the function of the satellite glial cells, but a recent study suggests that the satellite glial cell has a significant role in controlling the microenvironment in ganglia (Ohara et al., 2009). The satellite glial cells express the glutamate–aspartate transporter and glutamine synthetase (Miller et al., 2002) and may play an important role in maintaining glutamate homeostasis in the DRG (Bak et al., 2006). Another investigation implies the relevance between the satellite glial cells and the pain sensing mechanisms (Vit et al., 2008). Silencing of the inwardly rectifying potassium channels, which are expressed only in the satellite cells among DRG cells, results in appearance of both spontaneous and evoked pain and decreased tolerance to innocuous stimuli.

The major physiological role of Schwann cells is myelinating the axons of PNS neurons and thus facilitating the saltatory conduction. Schwann cells also contribute to the neuronal survival and nerve regeneration processes by providing neurotrophic factors (Madduri and Gander, 2010). After the denervation, Schwann cells produce many types of neurotrophic factors such as brain-derived neurotrophic factor, nerve growth factor (NGF), glial cell line-derived neurotrophic factor, which stimulate the axonal growth and support the neuronal survive (Shim and Ming, 2010).

Kai-Kai et al. (1986) have identified AVP immunoreactivity in neurons of rat DRG. Shortly after, a different group characterized the accumulation of inositol phosphates by application of AVP at concentrations in the micromolar range in rat DRG (Horn and Lightman, 1987), and this phenomenon was dependent on the V_1 AVP receptor subtype. Based on these studies, we could assume that: (i) AVP is also present in the PNS especially in neurons of the DRG and (ii) the inositol phosphate pathway is involved through receptors coupled to G_q proteins, suggesting the existence of AVP receptors in ganglia cells and the possibility for the peptides to induce the production of inositol 1,4,5-trisphosphate ($InsP_3$) responsible for the activation of Ca^{2+} release channels seated on the membrane of the endoplasmic reticulum. Within the huge family of 2nd messengers, Ca^{2+} is widely considered as the most ubiquitous and the control of Ca^{2+} homeostasis in cells is of major importance for the regulation of development, excitation, contraction, neurotransmitter release, aging and apoptosis (Thul et al., 2008). Taking all these aspects into consideration, the aim of the present study is to investigate the AVP-induced Ca^{2+} signaling in the cultured cells of the rat DRG. Our results show that AVP induces consistently a clear Ca^{2+} signal involving an $InsP_3$-evoked release of Ca^{2+} from the intracellular stores.

2. Results

2.1. AVP-induced $[Ca^{2+}]_i$ signals and immunoreactivity against S-100 in DRG cell culture

At six days in culture, various cell types were present in our DRG culture, that was distinguishable on morphological criteria (Fig. 1D). The first type was roundly shaped and had highly dense cytosol, resembling the morphology of the DRG neurons (Kitamura et al., 2005b) (a), while a second type was represented by polygonal or spindle shaped cells with lower density cytosol in phase contrast microscopy (b). To identify on a functional basis the types of cells, we have used a 60 mM KCl ($60K^+$) stimulation protocol (30 s) while performing $[Ca^{2+}]_i$ measurements. As illustrated in Fig. 1 A and B, showing an example of the $[Ca^{2+}]_i$ changes in a typical filed of the DRG culture, only one cell responded with a $[Ca^{2+}]_i$ increase to the $60K^+$-induced depolarization. Panel C in Fig. 1 shows the response of the culture to the bath application of 1 μM AVP for 1 min after the exposure to $60K^+$ for 30 s. The majority of the cells responded with a clear Ca^{2+} signal, while the neuronal cells failed to respond. This difference in response is more clearly illustrated by the $[Ca^{2+}]_i$ traces in panels F, where in a neuron (a) only $60K^+$ evoked a rapid sharp rise in $[Ca^{2+}]_i$, whereas in a non-neuronal cell (b), only AVP evoked a long-lasting $[Ca^{2+}]_i$ increase.

In the DRG, there are two types of glial cells, the satellite glial cells and Schwann cells, and both show the expression of the S-100 protein (Vega et al., 1991). Thus, to confirm the glial nature of the cells responding to AVP but not to $60K^+$

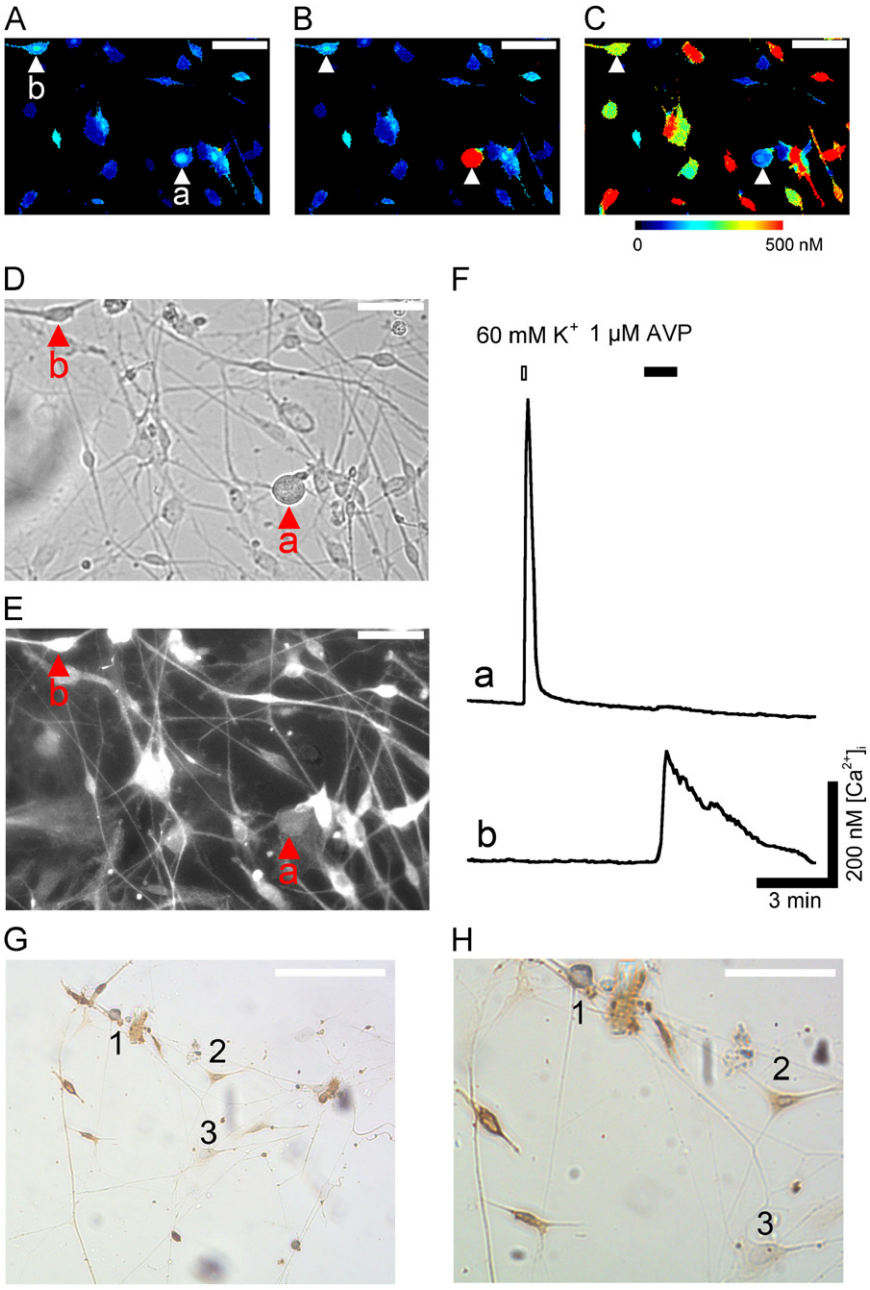

Fig. 1 – $[Ca^{2+}]_i$ responses to high K^+ and AVP with S-100 antibody immuno-staining in rat cultured DRG cells. (A)–(C) Ca^{2+} imaging pseudo color pictures obtained in basal conditions (A), after 60K^+ (B) and 1 μM AVP stimulations (C). (D) A bright field picture of the cells shown in A, B and C. (E) A fluorescence image obtained with anti S-100 antibody after the $[Ca^{2+}]_i$ dynamic measurement. (F) Time course of responses to K^+ and AVP obtained in the cells (a), (b), respectively (G), (H) Immunocytochemistry with an anti-S-100 antibody in DRG cells. Normal bright field images (G), (H) of the same optical field are shown. Cells numbered 1–3 in G are shown with an expanded scale in H. Only the cell 2 showed S-100-immunopositive. Scale bars indicate 50 (A)–(G) and 100 μm (H). The results of (A)–(F) and (G), (H) are obtained from the culture DRG cells at DIV 6 and DIV 3, respectively.

protocol in our DRG cultures on the basis of morphology and functional responses, we have performed immunocytochemical staining with an anti S-100 antibody on the coverslips previously used for $[Ca^{2+}]_i$ recording. As shown in the cell labeled 'b' in Fig. 1E, cells that responded to AVP were positively stained by the S-100 antibody. On the other hand, there was little S-100 immunoreactivity in the cell labeled 'a' that exhibited a transient rise in $[Ca^{2+}]_i$ to 60K^+.

To investigate the relative abundance of the S-100-immunopositive non-neuronal cells, we performed specific immunocytochemistry on the cultures. Under our experimental conditions, 71% (392/575) of cells having morphology of non-neuronal cells positively stained with S-100 antibody (Fig. 1G and H). More importantly, of the S-100 positive cells, 74% (103/139) responded with a Ca^{2+} signal to the application of AVP. Overall, these cells were quiescent in the absence of

stimulation, without signs of any spontaneous activities, such as $[Ca^{2+}]_i$ oscillations, and showed, under our Ca^{2+} calibration conditions, a resting $[Ca^{2+}]_i$ of 33.9±1.8 nM (n=832).

2.2. *Dependence of AVP-evoked $[Ca^{2+}]_i$ rises on the culture period and the AVP concentrations*

Maintenance of neural cells in primary cultures is usually associated with changes in the expression of various receptors, either as a function of the developmental stages or in response to the culture conditions (Abramov and Duchen, 2010; Costantini et al., 2010; Orlandi et al., 2011). To assess this possibility in our conditions, we have measured the amplitude of AVP-evoked (1 μM for 3 min) $[Ca^{2+}]_i$ responses and in cultures of different ages, between 0 and 10 DIV (days in vitro). For the sake of analysis, cells were divided into three groups depending on the amplitude of $[Ca^{2+}]_i$ increase in response to AVP: <10 nM (i.e., non-respondent), 10–30 nM (small responses) and >30 nM (large responses), and the relative proportion of these cell groups as a function of the age of the culture is plotted by columns in Fig. 2A. At DIV 0, 11% (35/331) of the cells showed responses larger than 30 nM, but the proportion of cells in this group gradually increased with the age in culture until DIV 4, and reached 72% (224/310). From the DIV 4 to DIV 10, the ratio of this group remained stable (approximately 70%). The average amplitudes of $[Ca^{2+}]_i$ responses in cells in the group showing responses larger than 30 nM in Fig. 2A are illustrated in Fig. 2B, demonstrating that the amplitude of the AVP-induced $[Ca^{2+}]_i$ response in the non-neuronal cells increased with culture age.

To examine the relationship between the concentration of AVP and the amplitude of the $[Ca^{2+}]_i$ responses, effects of AVP at different concentrations varying between 0.1 and 1000 nM on $[Ca^{2+}]_i$ were examined. To minimize the influence of the culture age on the amplitudes of AVP-induced responses, only DIV 9 cells were used in this experiment. Responses in individual cells were divided into three groups as Fig. 2A. Even at the low concentration (0.1 nM) of AVP, 16% of the cells showed $[Ca^{2+}]_i$ responses larger than 30 nM (Fig. 2C). The proportion of cells showing responses with the amplitude of larger than 30 nM gradually increased in a concentration-dependent manner. Fig. 2D shows the averaged amplitudes of the AVP-induced

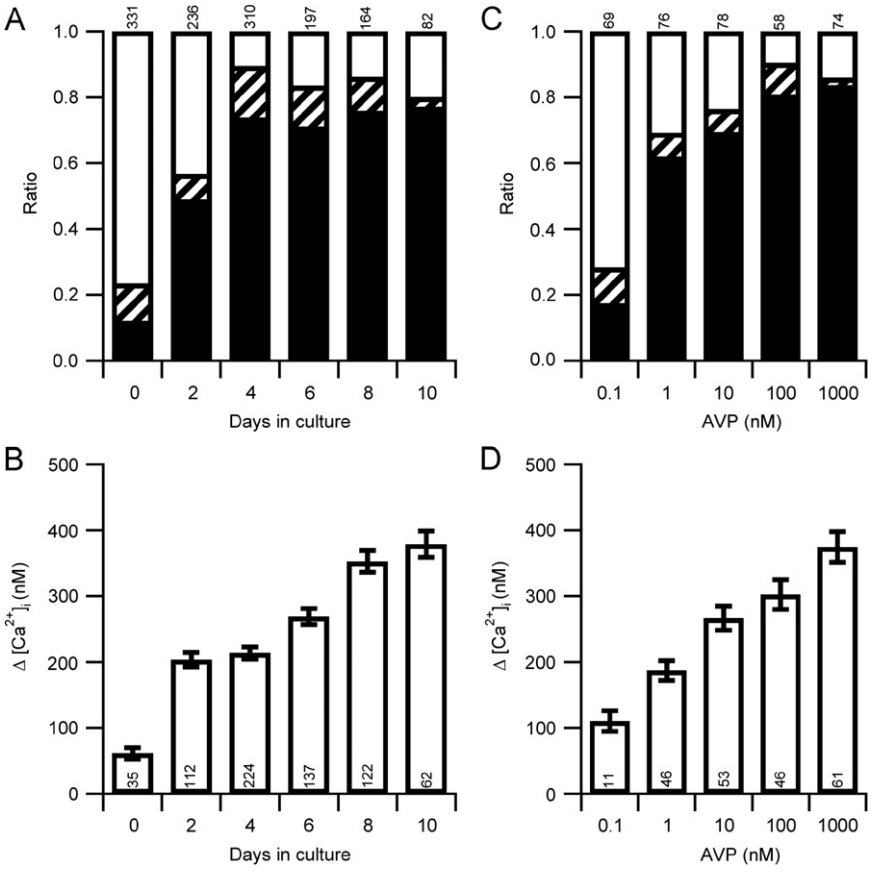

Fig. 2 – Dependence of AVP-evoked $[Ca^{2+}]_i$ responses on the culture day and the concentration of AVP. (A) Culture day dependence of AVP-evoked $[Ca^{2+}]_i$ responses in non-neuronal cells. Cells on each day of culture were divided into three groups depending on the amplitudes of the $[Ca^{2+}]_i$ responses as <10 nM (open column), 10–30 nM (hatched column), and >30 nM (solid column). (B) The mean amplitudes of the $[Ca^{2+}]_i$ responses in cells showing responses of >30 nM in A are shown. The total numbers of the cells in this group are indicated in the columns. (C) Dose dependence of AVP-evoked $[Ca^{2+}]_i$ responses in non-neuronal cells at DIV 9. Cells were divided into three groups as in A and the relative proportion of the cells in each group is shown by columns. (D) The mean amplitudes of the $[Ca^{2+}]_i$ responses in the cells showing responses of >30 nM in C are shown. The total numbers of the cells in this group are indicated in the columns. The amplitude of the $[Ca^{2+}]_i$ responses ($\Delta[Ca^{2+}]_i$) was calculated by subtracting the basal level from the peak amplitude of the evoked responses.

$[Ca^{2+}]_i$ increase in the group of the cells showing responses exceeding 30 nM as in Fig. 2C. The amplitudes also increased in a concentration-dependent manner.

2.3. $[Ca^{2+}]_i$ responses to repetitive stimulations with AVP

Assessment of the main parameters of Ca^{2+} homeostasis requires, in some experimental paradigms, repeated exposures to the activator agent. It has been shown previously that in the SON-AVP neurons, the $[Ca^{2+}]_i$ response to repeated stimulations with AVP shows desensitization (Dayanithi et al., 1996). A similar protocol was adopted in this study, involving 3 repetitive applications of a low, concentration of AVP (at 1 nM for 3 min), separated by 20 min intervals (Fig. 3A). Twenty-six out of 30 cells showed a good $[Ca^{2+}]_i$ response (i.e., larger than 30 nM) to all 3 repetitive applications of AVP. However, the $[Ca^{2+}]_i$ responses after the 1st and 2nd AVP applications were smaller suggesting a desensitization of the AVP receptors. The amplitudes of the $[Ca^{2+}]_i$ responses to the 1st, 2nd and 3rd stimulations were 231 ± 24 nM, 138 ± 9 nM, 90 ± 15 nM, respectively ($n=30$) and significantly different (1st and 2nd, $P<0.01$ by ANOVA; 2nd and 3rd, $P<0.05$ by ANOVA). Relative amplitudes of the responses to those evoked by the first stimulation are shown in Fig. 3B.

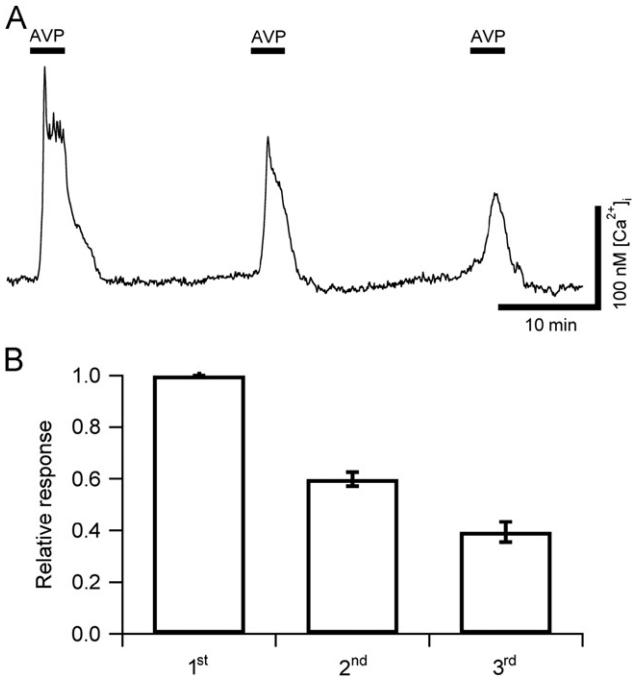

Fig. 3 – Effect of repetitive AVP stimulation on $[Ca^{2+}]_i$ in non-neuronal cells obtained from the DRG culture.
(A) Representative traces of $[Ca^{2+}]_i$ responses to 3 repetitive AVP applications (3 min each) with 20 min interval.
(B) Summarized results showing an amplitude decay of the $[Ca^{2+}]_i$ responses obtained from 30 non-neuronal cells.
The amplitude of the $[Ca^{2+}]_i$ responses (from the basal level to the peak) was normalized to the 1st $[Ca^{2+}]_i$ response and the values are shown as the mean ± SEM.

2.4. The source of Ca^{2+} in response to AVP

To clarify the origin of Ca^{2+} in response to AVP in the non-neuronal cells from DRG cultures, experiments were first performed to assess the response to AVP in the absence of external Ca^{2+}. For these experiments, cells were first stimulated with 1 nM AVP for 3 min (as shown in Fig. 4A) in the NL containing 2 mM $CaCl_2$ and then perfused with Ca^{2+}-free

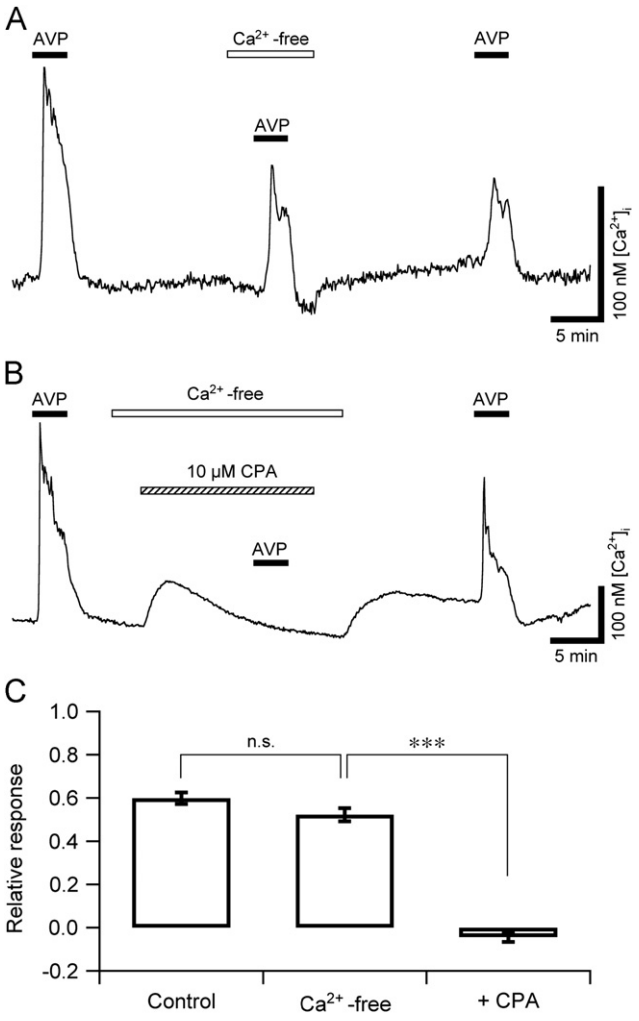

Fig. 4 – Involvement of external and intracellular Ca^{2+} in the AVP response. This panel displays the effects of low external Ca^{2+} and the sarco-endpalsmic reticulum Ca^{2+} ATPase inhibitor, CPA, on $[Ca^{2+}]_i$ responses to AVP in non-neuronal cells. (A) A representative trace showing $[Ca^{2+}]_i$ responses to AVP (1 nM) before, during, and after perfusion with Ca^{2+} free solution. (B) A representative example of $[Ca^{2+}]_i$ responses to AVP (1 nM) before, during, and after perfusion with CPA-containing Ca^{2+}-free solution.
(C) Summarized results showing $[Ca^{2+}]_i$ responses to AVP obtained in control ($n=30$), Ca^{2+} free ($n=40$), and Ca^{2+} free with CPA ($n=25$). Summarized data of control are obtained from the result of second time application of AVP in Fig. 3. The values are shown as the mean ± SEM. The $[Ca^{2+}]_i$ responses are expressed as relative responses in comparison to the 1st AVP-induced peak in each experiment (*: $P<0.001$).**

solution prior to 2nd application of AVP. The NL was then reintroduced as shown in the traces (Fig. 4). While data in Fig. 3B, show that the second AVP exposure induces a $[Ca^{2+}]_i$ response that is 60±2.7%, in the absence of external Ca^{2+}, the second response was 52±3% (n=40), a value that was not significantly different ($P>0.05$ by Student's t-test) from that recorded in the presence of Ca^{2+} (Fig. 4C), indicating that the AVP-induced Ca^{2+} signal originates in the intracellular Ca^{2+} compartments.

This is further supported in experiments using CPA, a drug known to block the reuptake of Ca^{2+} into the endoplasmic reticulum Ca^{2+} stores, but also to release Ca^{2+} from these stores in a manner controlled by the resting levels of $InsP_3$ (Bentley et al., 2010). In these experiments, CPA (10 μM) alone, in the absence of external Ca^{2+}, induced an sustained increase in $[Ca^{2+}]_i$, indicating of a release from the intracellular Ca^{2+} stores (Fig. 4B); and in these conditions AVP failed to initiate any $[Ca^{2+}]_i$ increase. However, when the Ca^{2+} concentration in the bath solution was restored to 2 mM, there was a prolonged rise in $[Ca^{2+}]_i$, which indicates a sustained store-operated Ca^{2+} entry (SOCE) was evoked, and the Ca^{2+} stores were refilled. In such conditions, a further AVP application is able to generate a transient $[Ca^{2+}]_i$ response; and these results are summarized in Fig. 4C.

The final indication that AVP generates a Ca^{2+} signal mediated by intracellular signaling involving $InsP_3$ and subsequent intracellular Ca^{2+} release, comes from experiments using modulators of phospholipase C (PLC) activity. The compound U73122 has been used extensively as a relatively specific inhibitor of PLC (Sabatier et al., 1998), while the related compound U73343 has no inhibitory activity (Smith et al., 1990). The cultures were thus exposed to AVP, and then pre-incubated with U73122 for 3 min prior to the 2nd AVP administration (Fig. 5A). While U73122 addition did not affected the levels of resting Ca^{2+}, it significantly reduced the AVP-evoked $[Ca^{2+}]_i$ rises (Fig. 5A and C); Fig. 5B and C shows that the non-specific agent U73343 had no effect.

2.5. *The subtype of AVP receptors contributing to the $[Ca^{2+}]_i$ rises*

In order to examine whether AVP-induced $[Ca^{2+}]_i$ responses in non-neuronal cells of DRG cell cultures are mediated by specific AVP receptors, we then pharmacologically targeted the subtypes of AVP receptor contributing to the $[Ca^{2+}]_i$ response by use of the V_1 receptor antagonist, (d(CH_2)$^1_5$, Tyr(Me)^2,Arg^8)-Vasopressin. Initially the cells were stimulated with a low AVP concentration (at 1 nM for 3 min) to identify the AVP-responsive cells; subsequently cells were stimulated by a much larger AVP concentration (1 μM, 3 min, n=25, control) (Fig. 6A). The rationale for the use of a much larger concentration of AVP for the secondary exposure was to counteract the desensitization effect. To test the effect of the antagonist, the cells were perfused with (d(CH_2)$^1_5$, Tyr(Me)^2,Arg^8)-Vasopressin at 100 nM for 3 min before the 2nd AVP stimulation, and continuously perfused further for 9 min. (d(CH_2)$^1_5$,Tyr(Me)^2,Arg^8)-Vasopressin alone had no effect on resting $[Ca^{2+}]_i$. In the presence of the antagonist, the $[Ca^{2+}]_i$ response evoked by AVP was completely abolished in all cells recorded (n=18, Fig. 6B) and there was a significant

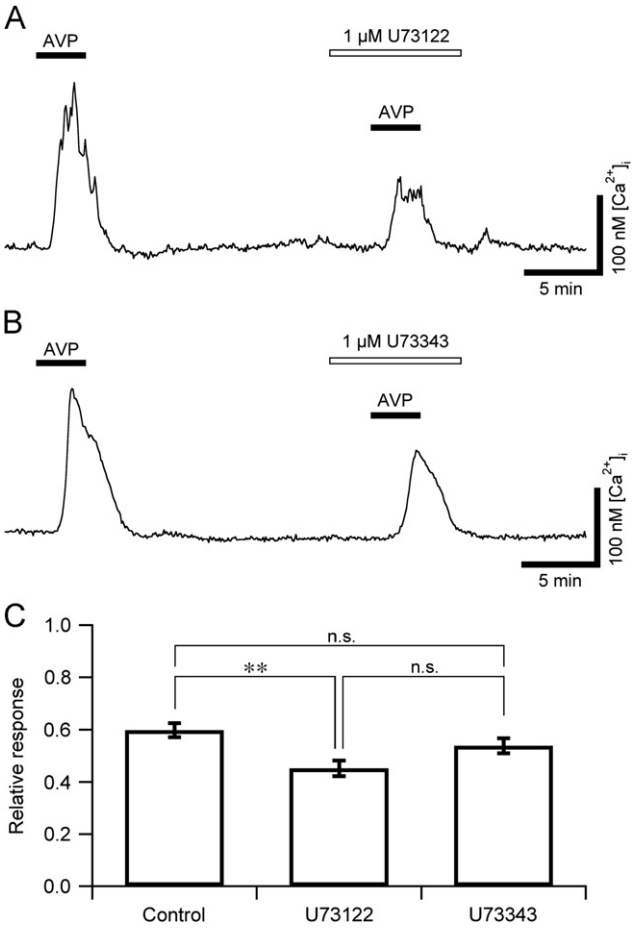

Fig. 5 – The possibility of PLC participation in the $[Ca^{2+}]_i$ responses evoked by AVP. This panel displays the effects of the PLC inhibitor, U73122 and inactive analog of U73122, U73343 on $[Ca^{2+}]_i$ responses to AVP in non-neuronal cells. (A), (B) Representative traces of $[Ca^{2+}]_i$ responses to AVP (1 nM) in the presence of U73122 (1 μM) or U73343 (1 μM). (C) Summarized results showing $[Ca^{2+}]_i$ responses to AVP obtained in U73122 (n=48), and U73343 (n=30). The values are shown as the mean±SEM. The $[Ca^{2+}]_i$ responses are expressed as relative responses in comparison to the 1st AVP-induced peak in each experiment (: $P<0.01$).**

difference between the amplitudes of AVP-evoked $[Ca^{2+}]_i$ responses in control cells and the ones obtained in the cells treated with (d(CH_2)$^1_5$,Tyr(Me)^2,Arg^8)-Vasopressin (tested by Student's t test; $P<0.05$). Since AVP at higher concentrations was shown to activate oxytocin (OT) receptors (Chini and Manning, 2007), we also examined the specificity of the involvement of AVP receptors by using the OT receptor antagonist, dOVT, on the $[Ca^{2+}]_i$ responses evoked by AVP in non-neuronal cells. Using the same protocols as, application of dOVT did not affect the AVP-evoked Ca^{2+} signal (tested by Student's t test; $P>0.05$ vs. control) (n=34, Fig. 6C) suggesting the specificity of action of AVP in non-neuronal cells in DRG.

To clarify the subtype of vasopressin receptors expressed in the DRG, RT-PCR was carried out. As shown in Fig. 7A, PCR products corresponding to V_{1a} and V_{1b} cDNAs were observed when using samples from rat DRG tissues, but no signal was

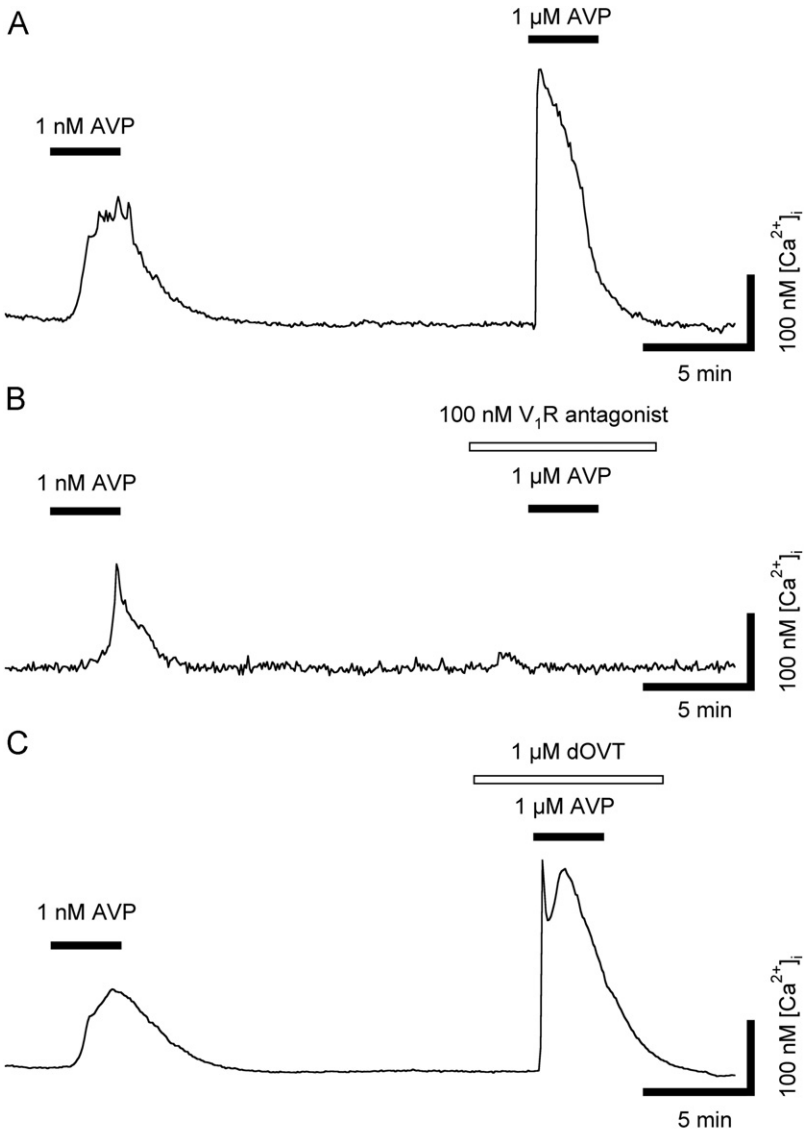

Fig. 6 – A specific subtype of vasopressin receptor mediates AVP-induced Ca^{2+} transients. This panel displays the effects of the V_1 receptor antagonist, (d(CH_2)$^1_5$,Tyr(Me)^2,Arg^8)-Vasopressin, and the effects of the OT receptor antagonist, dOVT, on $[Ca^{2+}]_i$ responses to AVP in non-neuronal cells. (A) Typical traces of $[Ca^{2+}]_i$ responses to AVP (1 and 1 μM) administered with 20 min intervals. (B) Representative traces of $[Ca^{2+}]_i$ responses to AVP (1 μM) in the presence of V_1 receptor antagonist, (d(CH_2)$^1_5$,Tyr(Me)^2,Arg^8)-Vasopressin (100 nM) (n=25) or an OT receptor antagonist, dOVT (1 μM) (C) (n=34).

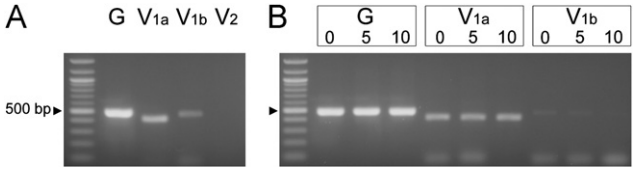

Fig. 7 – The expression of AVP receptor mRNAs in DRG tissues and cultured DRG cells. (A) The expression of V_{1a}, V_{1b} and V_2 receptor mRNAs in rat DRG tissue was analyzed by RT-PCR using the specific primers listed in Table 1. (B) The expression of GAPDH (G), V_{1a} and V_{1b} receptor mRNAs in cultured DRG cells at DIV 0, 5 and 10.

detected with the V_2 receptor primers. Because amplitudes of $[Ca^{2+}]_i$ responses evoked by AVP increased during culture days in our study (Fig. 2B), we also examined culture-day-dependent changes in expressions of mRNAs in cultured DRG cells (Fig. 7b). V_{1a} receptor mRNA was expressed in cultured DRG cells at DIV 0, 5 and 10. In contrast, weak signal of V_{1b} mRNA in cells at DIV 0 and 5 was observed weakly and no signal was detected in cells at DIV 10.

3. Discussion

Although the presence of AVP and of a neuropeptidergic system in DRG has been known for some time (Horn and Lightman, 1987; Kai-Kai et al., 1986) there are no detailed studies of the possible effects and signaling pathways evoked by involvement AVP. Therefore the purpose of this work was to elucidate how various types of DRG cells, specifically

non-neuronal cells, could respond to the challenges of AVP in terms of Ca^{2+} handling.

3.1. AVP induces $[Ca^{2+}]_i$ transients in cultured DRG glial cells

We demonstrated that DRG cells showed rapid $[Ca^{2+}]_i$ responses to AVP in a concentration-dependent manner in the physiological range. The results of the immunocytochemical staining in combination with the $[Ca^{2+}]_i$ measurement revealed that the majority of the non-neuronal cells having high sensitivity to AVP in the DRG was S-100-immunopositive. It has been reported that the two types of glial cells in the DRG are S-100-immunopositive (Vega et al., 1991). Taken together, it is considered the cells that did not respond to $60K^+$ but responded to AVP in the present study are most likely to be either satellite glial cells or Schwann cells.

The minimum effective concentrations of AVP causing $[Ca^{2+}]_i$ responses were 100 pM in non-neuronal cells in DRG culture. This concentration is close to that reported for AVP-evoked $[Ca^{2+}]_i$ responses in hippocampal and cortical astrocytes (Syed et al., 2007).

3.2. AVP receptor subtype

Our pharmacological approach led us to identify important features of the $[Ca^{2+}]_i$ response evoked by AVP. This response shows a significant desensitization. The AVP-evoked $[Ca^{2+}]_i$ response was completely blocked by the selective V_1 antagonist, $(d(CH_2)^1_5,Tyr(Me)^2,Arg^8)$-Vasopressin, and unaffected by the selective OT receptor antagonist, dOVT, indicating that AVP receptors mediating the $[Ca^{2+}]_i$ response are the V_1 subclass. The AVP-evoked $[Ca^{2+}]_i$ response showed clear desensitization when AVP was administered repeatedly. The results are consistent with previous reports that cellular responses via V_1 AVP receptors undergo strong desensitization in AVP-evoked $[Ca^{2+}]_i$ responses from smooth muscle cells of rat aorta (Briner et al., 1992; Schrier et al., 1993) porcine retinal arteries (Caramelo et al., 1991), secretory responses from ovine pituitary corticotrophs (Hassan et al., 2003; Hassan and Mason, 2005), and SON-AVP neurons (Dayanithi et al., 1996; Gouzenes et al., 1999).

V_{1a} and V_{1b} PCR products were observed when using samples from DRG tissues, suggesting that both V_{1a} and V_{1b} receptor mRNAs are expressed in rat DRG tissues. In cultured DRG cells prepared by the same method as used for cell isolation for the $[Ca^{2+}]_i$ measurement, clear V_{1a} PCR products were observed sustainably during the culture days, but a weak V_{1b} PCR signal was observed at DIV 0 and 5, and no signal was observed at DIV10. Considering the larger $[Ca^{2+}]_i$ responses in the later culture days, these results indicate that the AVP receptor subtype responsible for the $[Ca^{2+}]_i$ responses in rat DRG culture cells may be the V_{1a} subtype.

3.3. Signal transduction mechanism of AVP receptors in the DRG

The V_1 receptor is known to be coupled to Gq/11 proteins, which activate PLC and lead to the production of $InsP_3$ (Viero et al.). Several lines of the argument supports the view that the AVP-evoked Ca^{2+} signals in the DRG glial cells are mediated by an $InsP_3$-dependent signaling pathway: (i) the response was not affected by the removal of extracellular Ca^{2+} but (ii) abolished by the release from the intracellular Ca^{2+} stores with CPA, and (iii) the PLC blocker U-73122 inhibited AVP-evoked $[Ca^{2+}]_i$ rises. Presence of PLC has been reported in DRG neurons (Han et al., 2006; Joseph et al., 2007; Lagercrantz et al., 1995) with all the major PLC isoforms beta1, beta3 and beta4 being expressed, although there appear to be a prevalence of the beta3 isoform (Han et al., 2006), which has been shown to play a critical role in neuropathic pain in mouse and human DRG (Shi et al., 2008). The present results indicate the existence PLC also in the DRG glial cells, although little is known about the isoform expressed.

The Gq-PLC-$InsP_3$ mechanism is well known to evoke $InsP_3$-dependent Ca^{2+} release from intracellular Ca^{2+} stores, and Ca^{2+} store depletion due to massive Ca^{2+} release has been shown to activate store-operated Ca^{2+} entry (SOCE) through plasma membrane Ca^{2+} channels (Parekh and Putney, 2005). The present results that a prolonged $[Ca^{2+}]_i$ increase was observed upon CPA removal and extracellular Ca^{2+} restoration indicates such mechanism is present also in DRG glial cells. Activation of SOCE could be one of the reasons why AVP-evoked $[Ca^{2+}]_i$ responses in glial cells showed very slow recovery when a high concentration of AVP was applied (Fig. 1F).

3.4. Possible physiological roles of AVP in DRG

The probable sources of AVP to activate V_1 receptors of non-neuronal cells in the DRG are the neurons themselves (Kai-Kai et al., 1986) but the circulating AVP could also have an effect. It has been documented that, in the hypophysial portal blood, the plasmatic AVP concentration is around 0.5 nM (Link et al., 1992). In other models, Lee and collaborators reported a physiological concentration of AVP of 50–100 pg/ml (46–92 pM) in the heart (Lee et al., 2003), and physiological effects of AVP were seen at 3–30 pM in the pancreas of the rat (Yibchok-Anun et al., 1999). Circulating AVP concentration changes mainly during dehydration and it has been reported that over 48–72 h of dehydration condition, plasma AVP concentration increases more than 10 times above basal levels (Steiner and Phillips, 1988; Terada et al., 1993). Therefore it would be plausible that AVP concentrations similar to those used in our study to elicit Ca^{2+} signals could be found in physiological states. If AVP was released from DRG neurons themselves, the AVP concentration in the DRG would reach a much higher level than that discussed above, and thus be even more likely to induce a Ca^{2+} signal in neighboring glial cells.

Local functional regulation by small peptidetgic signaling is not uncommon. Bradykinin (BK), another nonapeptide, has been shown to cause a $[Ca^{2+}]_i$ signal in DRG Schwann cells, with a release of glutamate and aspartate (Parpura et al., 1995). The BK-evoked increase of $[Ca^{2+}]_i$ in satellite glial cells from postnatal DRG also activate a Ca^{2+}-dependent Cl^- conductance, with a putative participation in the inflammatory process (England et al., 2001). Moreover, AVP has been shown to elevate $[Ca^{2+}]_i$ and release glutamate in hippocampal and cortical astrocytes of rats (Syed et al., 2007). Whether or not

AVP can have similar effects and induce a glial release of bioactive substances in the DRG remains to be determined.

In the present study, the amplitude of $[Ca^{2+}]_i$ responses evoked by AVP (1 μM) increased with an increase in the culture time. Even under an acute condition (day 0), about 10% of cells examined showed $[Ca^{2+}]_i$ responses larger than 30 nM upon AVP application, indicating that the AVP-mediated $[Ca^{2+}]_i$ response of glial cells in the DRG could exist also in vivo. Moreover, if AVP was released from neighboring DRG neurons, the concentration of AVP would reach a level much higher than the level of AVP in the systemic circulation discussed above, and it would be sufficient to evoke the $[Ca^{2+}]_i$ response in DRG glial cells. At day 0, the mean amplitude of $[Ca^{2+}]_i$ responses obtained from the group showing responses larger than 30 nM was six times smaller than that obtained at day 10. The differences in the amplitudes of the $[Ca^{2+}]_i$ responses due to culturing time could result from differences in the expression density of the AVP V_1 receptor on the plasma membrane. There are at least two possibilities that the density of V_1 receptor expressed at day 0 could be low: (1) V_1 receptors are highly expressed on the glial cells in vivo but internalized or damaged during the enzymatic and mechanical digestions, and recover during cell culture; (2) The density of V_1 receptors expressed on the glial cells increases during the day of cell culture. Our RT-PCR results showed that V_{1a} receptor mRNA was strongly expressed both in DRG tissues and in cultured DRG cells even at culture day 0, and that there was no evident change in the expression during culture. These results support the first possibility.

With this communication we show that the neuropeptide AVP generates Ca^{2+} signals in DRG glial cells, in a concentration-dependent and receptor-specific manner. This suggests that the vasopressinergic molecular machinery could play a role in the physiology and/or pathophysiology of the peripheral sensory system.

4. Experimental procedures

4.1. DRG cell isolation and culture

DRG cells were isolated from adult male Sprague-Dawley rats (7–12 weeks old), using the procedures reported previously (Kitamura et al., 2005a; Komagiri and Kitamura, 2003; Ozaki et al., 2009). Animals were sacrificed according to the guidelines of the ethical committee of Tottori University, Japan. The rats were killed by cervical dislocation under anesthesia by an intraperitoneal injection of pentobarbital (5 mg/kg bw). Ganglia were dissected from the entire length of the vertebral column. Axons extending from the ganglia were removed under a stereoscopic microscope. The ganglia were incubated in Ca^{2+}/Mg^{2+}-free phosphate-buffered saline (PBS) containing 300 U/ml collagenase type IV (Worthington Biochemical, Lakewood, NJ, USA), 0.12 μg/ml DNase I and 1 mg/ml BSA for 2 h at 37 °C and then rinsed with PBS to remove the enzymes. They were then incubated in PBS containing 0.25% trypsin (Life technologies, California, USA) and 1 mg/ml BSA for 15 min at 37 °C. After the enzymatic digestion, the cells were gently triturated with a silicon-coated Pasteur pipette and centrifuged at 1000 rpm for 5 min to remove the enzymes. The cells were suspended in DMEM (Life technologies) with glucose (4.5 g/l) and plated onto coverslips (11 mm in diameter) coated with 50 mg/ml poly-D-lysine. The cells were kept at 37 °C in a humidified atmosphere of 95% air and 5% CO_2 until use. The DMEM was supplemented with 10% FBS (MP Biochemicals, Irvine, CA, USA), 100 U/ml penicillin (Life technologies), 100 μg/ml streptomycin (Life technologies) and 5 μM cytosine-β-D-arabinofuranoside. The culture medium was changed every 2 day. The $[Ca^{2+}]_i$ measurements were performed between the 5th and 11th day of culture.

4.2. $[Ca^{2+}]_i$ measurements

The $[Ca^{2+}]_i$ in cultured rat DRG cells was measured with Fura-2, a fluorescent Ca^{2+} indicator, according to the procedure reported previously (Ozaki et al., 2009). The cultured cells were incubated in HEPES-buffered Normal Locke's solution (NL; in mM: 140 NaCl, 5 KCl, 2 $CaCl_2$, 1.2 $MgCl_2$, 10 glucose, 10 HEPES, pH was adjusted to 7.4 with Tris; the osmolarity was between 298 and 300 mOsmol/l) containing 2 μM Fura-2/AM (Merck, Whitehouse Station, NJ, USA) and 0.01% Pluronic acid F-127 (Life technologies) for 60 min at room temperature (22–24 °C) in the dark. After the incubation, the coverslip was mounted onto the recording chamber (RC-25F, Warner Instruments, Hamden, USA) which is fixed on the stage of an inverted fluorescence microscope (IX71, Olympus, Tokyo, Japan). The cells were continuously perfused with solutions containing various experimental drugs through polypropylene tubes connected to a peristaltic pump (Minipuls 3, Gilson, Middleton, WI, USA) at a flow rate of 1.4 ml/min. In this system, the solution around the cells could be changed rapidly within a few seconds. The Fura-2 fluorescence signal was detected through a UV objective lens (UApo 20 × 3/340, Olympus), and the florescence image passing through a band-pass filter (500±10 nm) was captured by a cooled CCD camera (ORCA-ER, Hamamatsu Photonics). All experiments were performed at room temperature (22–24 °C).

4.3. Data acquisition and analysis

Data acquisition was made according to the procedure reported previously (Ozaki et al., 2009). Briefly, Fura-2 images were captured at a sampling frequency of 0.2 Hz using Aqua Cosmos software (Hamamatsu Photonics). The fluorescent intensity at the excitation wavelengths of 340 (F340) and 380 nm (F380) was determined by the analyzing software (Aqua Cosmos, Hamamatsu Photonics). The ratio of fluorescence for each pixel obtained with the excitation at 340 and 380 nm (F340/F380) was used to calculate $[Ca^{2+}]_i$. A calibration curve of $[Ca^{2+}]_i$ for F340/F380 was determined using a series of Ca^{2+}-buffered solutions (Life technologies). To estimate the $[Ca^{2+}]_i$ levels in individual cells, regions of interest (ROIs) were chosen to include the soma of each DRG cell, and average values for $[Ca^{2+}]_i$ in pixels contained in each ROI were calculated. The amplitude of $[Ca^{2+}]_i$ responses was expressed as $\Delta[Ca^{2+}]_i$, which was calculated by subtracting average $[Ca^{2+}]_i$ levels during 2 min before AVP application from peak $[Ca^{2+}]_i$ amplitudes detected during 5 min after the onset of AVP application. Changes in the calculated $[Ca^{2+}]_i$ were analyzed by IGOR Pro (Wavemetrics, Lake Oswego, OR,

Table 1 – Primers for RT-PCR.

Gene	Sequence	Product size (bp)	Reference
V_{1a} receptor	GCGGAAAGACAGCGTCCTCGCGACA GCTCATGCTATCGGAGTCATCCTTGGCGAAT	416	(Chritin et al., 1999)
V_{1b} receptor	GTCAGCAGCATCAGTACCATCTCCAGCGCA CATAGTGGCTTCCCCGTCCACCTGCTCTA	462	(Chritin et al., 1999)
V_2 receptor	TACCTGCAGATGGTGGGCAT AGCAACACAAAGGGGGGTCT	581	(Machida et al., 2007)
GAPDH	AGTCGGAGTGAACGGATTTGG AGTTGTCATGGATGACCTTGG	488	

USA) and Excel (Microsoft, Redmond, WA, USA). Data are presented as the means ± SEM. The statistical significance was assessed by One-factor analysis of variance (ANOVA) or Student's *t*-test. Differences were considered statistically significant if $P<0.05$.

4.4. *Immunocytochemistry*

After the $[Ca^{2+}]_i$ measurements, the cells on some coverslips were analyzed for fluorescent immunocytochemistry to distinguish glial cells from other types of cells. All staining processes were made in the recording chamber keeping the observation field of the $[Ca^{2+}]_i$ measurement. After the $[Ca^{2+}]_i$ measurement, cells on the coverslips were perfused with PBS for 5 min and then fixed with PBS containing 4% paraformaldehyde (PFA) for 15 min. After the fixation, the cells were perfused with PBS for 5 min to remove PFA and then permeabilized with PBS containing 0.1% Triton X-100 for 5 min. They were then perfused with PBS for 5 min and perfused with the blocking solution that consisted of PBS containing 10% donkey serum for 30 min. After the blocking, the cells were probed by the rabbit anti-bovine S-100 polyclonal antibody (dilution: 1:50; AbD Serotec, Kidlington, UK) for 12–15 h. Then the primary antibody was removed by perfusing the cells with PBS for 5 min. During this step, auto-fluorescence of the cells, those used for the $[Ca^{2+}]_i$ measurements, was captured by the CCD camera. Then, cells were probed with the secondary antibody, the donkey anti-rabbit IgG antibody (dilution: 1:300) conjugated with Alexa 488 (Life technologies). They were then mounted on the chamber to label anti-S-100 antibody for 1 h. Finally, the stained cells were perfused with PBS for 5 min, and fluorescence images of Alexa 488 were captured by the CCD camera.

In addition to the fluorescent immunocytochemistry, S-100-immunopositive cells were detected by the enzymatic immunocytochemistry, the procedures which have been reported previously (Kitamura et al., 2005a). In brief, after the blocking with 10% goat serum in PBS, the cells were probed by the anti-S100 antibody (dilution: 1:50; AbD Serotec) for 12–15 h. Then primary antibody was washed with PBS and cells were probed with the secondary antibody, HRP-conjugated goat anti-rabbit IgG antibody (dilution: 1:200) for 2 h. Finally, the probed cells were visualized by 3,3′-diaminobenzidine tetrahydrochloride (1 mg/ml) for 10 min and were counter stained with hematoxyline. All immunocytochemical experiments were performed at room temperature (22–24 °C).

4.5. *RNA isolation and RT-PCR*

Total RNAs used for reverse transcription-polymerase chain reaction (RT-PCR) were isolated from DRG tissues and cultured DRG cells using Trizol reagent (Life technologies) according to the manufacture's protocol. Reverse transcription was performed with 1 μg (DRG tissue) and 0.4 μg (cultured DRG cells) total RNA using PrimeScript RT-PCR Kit (Takara Bio Inc., Shiga, Japan) according to the manufacture's protocol. PCR was performed with 1 μl of first-strand cDNA, a primer pair listed in Table 1 and Emerald Amp MAX PCR Master Mix (Takara Bio). The PCR profile was as follows: 94 °C for 30 s, 60 °C for 30 s, 72 °C for 30 s, for 30 cycles. After amplification, PCR products and 100 bp DNA ladder (New England Ipswich, MA, USA) were electrophoresed with TAE buffer on a 1.5% agarose gel (Bio-Rad laboratories, Inc., California, USA) containing 1 μg/ml ethidium bromide. Bands were excited by ultraviolet light and photographed.

4.6. *Solutions and drugs*

A solution containing high K^+ (60 mM) was made by the isotonic replacement of Na^+ of HEPES-buffered NL with K^+. A Ca^{2+}-free solution was made by simply omitting $CaCl_2$ from the NL. A concentrated stock solution of cyclopiazonic acid (CPA), an inhibitor of the Ca^{2+}-ATPase of the intracellular Ca^{2+} store (Seidler et al., 1989), at 10 mM were made in dimethyl sulfoxide and stored at −30 °C until use. A concentrated stock solution of [Arg^8]-Vasopressin (Peptide Institute, Osaka, Japan) at 0.1 mM, ($d(CH_2)^1_5$,$Tyr(Me)^2$,Arg^8)-Vasopressin, a receptor antagonist of V_1 and ($d(CH_2)^1_5$,$Tyr(Me)^2$,Thr^4, Orn^8,des-Gly-NH^9_2)-Vasotocin (dOVT), a receptor antagonist of OT (BACHEM, Bubendorf, Switzerland) at 1 mM were made in double distilled water and stored at −30 °C until use. All standard chemicals were from Sigma-Aldrich, St Louis, MO, USA, unless stated otherwise.

Acknowledgments

This study was supported by KAKENHI (Grant #: 16780200 and 18380175) and the Grant Agency of the Czech Republic grants GA CR P303/11/0192. E.C. Toescu and G. Dayanithi were supported by the Japanese Society for Promotion of Science Invitation Fellowship Program (Grant #: S-09105 and S-10200).

REFERENCES

Abramov, A.Y., Duchen, M.R., 2010. Impaired mitochondrial bioenergetics determines glutamate-induced delayed calcium deregulation in neurons. BBA 1800, 297–304.

Bak, L.K., Schousboe, A., Waagepetersen, H.S., 2006. The glutamate/GABA-glutamine cycle: aspects of transport, neurotransmitter homeostasis and ammonia transfer. J. Neurochem. 98, 641–653.

Bentley, M., Nycz, D.C., Joglekar, A., Fertschai, I., Malli, R., Graier, W.F., Hay, J.C., 2010. Vesicular calcium regulates coat retention, fusogenicity, and size of pre-Golgi intermediates. Mol. Biol. Cell 21, 1033–1046.

Bielsky, I.F., Hu, S.B., Szegda, K.L., Westphal, H., Young, L.J., 2004. Profound impairment in social recognition and reduction in anxiety-like behavior in vasopressin V_{1a} receptor knockout mice. Neuropsychopharmacology: official publication of the American College of Neuropsychopharmacology 29, 483–493.

Bone, E., Fretten, P., Palmer, S., Kirk, C., Michell, R., 1984. Rapid accumulation of inositol phosphates in isolated rat superior cervical sympathetic ganglia exposed to V_1-vasopressin and muscarinic cholinergic stimuli. Biochem. J. 221, 803–811.

Briner, V.A., Williams, B., Tsai, P., Schrier, R.W., 1992. Demonstration of processing and recycling of biologically active V_1 vasopressin receptors in vascular smooth muscle. Proc. Nat. Acad. Sci. U.S.A. 89, 2854–2858.

Caramelo, C., Tsai, P., Okada, K., Briner, V.A., Schrier, R.W., 1991. Mechanisms of rapid desensitization to arginine vasopressin in vascular smooth muscle cells. Am. J. Physiol. 260, F46–F52.

Chini, B., Manning, M., 2007. Agonist selectivity in the oxytocin/vasopressin receptor family: new insights and challenges. Biochem. Soc. Trans. 35, 737–741.

Chritin, M., Roquette, P., Schulz, M.F., Breton, C., Tribollet, E., 1999. Up-regulation of vasopressin V(1a) receptor mRNA in rat facial motoneurons following axotomy. Brain Res. Mol. Brain Res. 70, 210–218.

Costantini, C., Lorenzetto, E., Cellini, B., Buffelli, M., Rossi, F., Della-Bianca, V., 2010. Astrocytes regulate the expression of insulin-like growth factor 1 receptor (IGF1-R) in primary cortical neurons during in vitro senescence. J. Mol. Neurosci.: MN 40, 342–352.

Dayanithi, G., Widmer, H., Richard, P., 1996. Vasopressin-induced intracellular Ca^{2+} increase in isolated rat supraoptic cells. J. Physiol. 490 (Pt 3), 713–727.

Dayanithi, G., Viero, C., Shibuya, I., 2008. The role of calcium in the action and release of vasopressin and oxytocin from CNS neurones/terminals to the heart. J. Physiol. Pharmacol. 59 (8), 7–26.

England, S., Heblich, F., James, I., Robbins, J., Docherty, R., 2001. Bradykinin evokes a Ca^{2+}-activated chloride current in non-neuronal cells isolated from neonatal rat dorsal root ganglia. J. Physiol. 530, 395–403.

Gouzenes, L., Sabatier, N., Richard, P., Moos, F.C., Dayanithi, G., 1999. V_{1a}- and V_2-type vasopressin receptors mediate vasopressin-induced Ca^{2+} responses in isolated rat supraoptic neurones. J. Physiol. 517 (Pt 3), 771–779.

Han, S.K., Mancino, V., Simon, M.I., 2006. Phospholipase Cbeta 3 mediates the scratching response activated by the histamine H1 receptor on C-fiber nociceptive neurons. Neuron 52, 691–703.

Hanani, M., 2005. Satellite glial cells in sensory ganglia: from form to function. Brain Res. Brain Res. Rev. 48, 457–476.

Hassan, A., Chacko, S., Mason, D., 2003. Desensitization of the adrenocorticotrophin responses to arginine vasopressin and corticotrophin-releasing hormone in ovine anterior pituitary cells. J. Endocrinol. 178, 491–501.

Hassan, A., Mason, D., 2005. Mechanisms of desensitization of the adrenocorticotropin response to arginine vasopressin in ovine anterior pituitary cells. J. Endocrinol. 184, 29–40.

Horn, A., Lightman, S., 1987. Vasopressin-induced turnover of phosphatidylinositol in the sensory nervous system of the rat. Exp. Brain Res. 68, 299–304.

Jessen, K.R., Mirsky, R., 2005. The origin and development of glial cells in peripheral nerves. Nat. Rev. Neurosci. 6, 671–682.

Joseph, E.K., Bogen, O., Alessandri-Haber, N., Levine, J.D., 2007. PLC-beta 3 signals upstream of PKC epsilon in acute and chronic inflammatory hyperalgesia. Pain 132, 67–73.

Kai-Kai, M., Anderton, B., Keen, P., 1986. A quantitative analysis of the interrelationships between subpopulations of rat sensory neurons containing arginine vasopressin or oxytocin and those containing substance P, fluoride-resistant acid phosphatase or neurofilament protein. Neuroscience 18, 475–486.

Karashima, T., 1981. Effects of vasopressin on smooth muscle cells of guinea-pig mesenteric vessels. Br. J. Pharmacol. 72, 673–684.

Kitamura, N., Konno, A., Kuwahara, T., Komagiri, Y., 2005a. Nerve growth factor-induced hyperexcitability of rat sensory neuron in culture. Biomed. Res. 26, 123–130.

Kitamura, N., Konno, A., Kuwahara, T., Komagiri, Y., 2005b. Nerve growth factor-induced hyperexcitability of rat sensory neuron in culture. Biomed. Res. 26, 123–130.

Komagiri, Y., Kitamura, N., 2003. Effect of intracellular dialysis of ATP on the hyperpolarization-activated cation current in rat dorsal root ganglion neurons. J. Neurophysiol. 90, 2115–2122.

Lagercrantz, J., Piehl, F., Nordenskjold, M., Larsson, C., Weber, G., 1995. Expression of the phosphoinositide-specific phospholipase Cbeta3 gene in the rat. Neuroreport 6, 2542–2544.

Le Douarin, N., Dulac, C., Dupin, E., Cameron-Curry, P., 1991. Glial cell lineages in the neural crest. Glia 4, 175–184.

Lechner, S., Frenzel, H., Wang, R., Lewin, G., 2009. Developmental waves of mechanosensitivity acquisition in sensory neuron subtypes during embryonic development. EMBO J. 28, 1479–1491.

Lee, C., Watkins, M., Patterson, J., Gattis, W., O'connor, C., Gheorghiade, M., Adams, K.J., 2003. Vasopressin: a new target for the treatment of heart failure. Am. Heart J. 146, 9–18.

Li, Y., Shiels, A.J., Maszak, G., Byron, K.L., 2001. Vasopressin-stimulated Ca^{2+} spiking in vascular smooth muscle cells involves phospholipase D. Am. J. Physiol. Heart C. 280, H2658–H2664.

Link, H., Dayanithi, G., Föhr, K., Gratzl, M., 1992. Oxytocin at physiological concentrations evokes adrenocorticotropin (ACTH) release from corticotrophs by increasing intracellular free calcium mobilized mainly from intracellular stores. Oxytocin displays synergistic or additive effects on ACTH-releasing factor or arginine vasopressin-induced ACTH secretion, respectively. Endocrinology 130, 2183–2191.

Machida, K., Wakamatsu, S., Izumi, Y., Yosifovska, T., Matsuzaki, T., Nakayama, Y., Kohda, Y., Inoue, T., Saito, H., Tomita, K., Nonoguchi, H., 2007. Downregulation of the V2 vasopressin receptor in dehydration: mechanisms and role of renal prostaglandin synthesis. Am. J. Physiol. Renal Physiol. 292, F1274–F12782.

Madduri, S., Gander, B., 2010. Schwann cell delivery of neurotrophic factors for peripheral nerve regeneration. JPNS 15, 93–103.

Manning, M., Stoev, S., Chini, B., Durroux, T., Mouillac, B., Guillon, G., 2008. Peptide and non-peptide agonists and antagonists for the vasopressin and oxytocin V_{1a}, V_{1b}, V_2 and OT receptors: research tools and potential therapeutic agents. Prog. Brain Res. 170, 473–512.

Miller, K.E., Richards, B.A., Kriebel, R.M., 2002. Glutamine-, glutamine synthetase-, glutamate dehydrogenase- and pyruvate carboxylase-immunoreactivities in the rat dorsal root ganglion and peripheral nerve. Brain Res. 945, 202–211.

Ohara, P.T., Vit, J.P., Bhargava, A., Romero, M., Sundberg, C., Charles, A.C., Jasmin, L., 2009. Gliopathic pain: when satellite glial cells go bad. The Neuroscientist: Rev. J. Neurobiol., Neurol. Psychiatry 15, 450–463.

Orlandi, C., La Via, L., Bonini, D., Mora, C., Russo, I., Barbon, A., Barlati, S., 2011. AMPA receptor regulation at the mRNA and protein level in rat primary cortical cultures. PloS one 6, e25350.

Ozaki, Y., Kitamura, N., Tsutsumi, A., Dayanithi, G., Shibuya, I., 2009. NGF-induced hyperexcitability causes spontaneous fluctuations of intracellular Ca^{2+} in rat nociceptive dorsal root ganglion neurons. Cell Calcium. 45, 209–215.

Pannese, E., 1981. The satellite cells of the sensory ganglia. Adv. Anat., Embryol. Cell Biol. 65, 1–111.

Parekh, A.B., Putney Jr., J.W., 2005. Store-operated calcium channels. Physiol. Rev. 85, 757–810.

Parpura, V., Liu, F., Jeftinija, K., Haydon, P., Jeftinija, S., 1995. Neuroligand-evoked calcium-dependent release of excitatory amino acids from Schwann cells. J. Neurosci. 15, 5831–5839.

Sabatier, N., Richard, P., Dayanithi, G., 1998. Activation of multiple intracellular transduction signals by vasopressin in vasopressin-sensitive neurones of the rat supraoptic nucleus. J. Physiol. 513 (Pt 3), 699–710.

Schrier, R.W., Briner, V., Caramelo, C., 1993. Cellular action and interactions of arginine vasopressin in vascular smooth muscle: mechanisms and clinical implications. J. Am. Soc. Nephrol. 4, 2–11.

Scroggs, R.S., Fox, A.P., 1992. Calcium current variation between acutely isolated adult rat dorsal root ganglion neurons of different size. J. Physiol. 445, 639–658.

Seidler, N.W., Jona, I., Vegh, M., Martonosi, A., 1989. Cyclopiazonic acid is a specific inhibitor of the Ca^{2+}-ATPase of sarcoplasmic reticulum. J. Biol. Chem. 264, 17816–17823.

Shi, T.J., Liu, S.X., Hammarberg, H., Watanabe, M., Xu, Z.Q., Hokfelt, T., 2008. Phospholipase C{beta}3 in mouse and human dorsal root ganglia and spinal cord is a possible target for treatment of neuropathic pain. Proc. Nat. Acad. Sci. U.S.A. 105, 20004–20008.

Shim, S., Ming, G.L., 2010. Roles of channels and receptors in the growth cone during PNS axonal regeneration. Exp. Neurol. 223, 38–44.

Smith, R.J., Sam, L.M., Justen, J.M., Bundy, G.L., Bala, G.A., Bleasdale, J.E., 1990. Receptor-coupled signal transduction in human polymorphonuclear neutrophils: effects of a novel inhibitor of phospholipase C-dependent processes on cell responsiveness. J. Pharmacol.Exp. Ther. 253, 688–697.

Steiner, M., Phillips, M.I., 1988. Renal tubular vasopressin receptors downregulated by dehydration. Am. J. Physiol. 254, C404–C410.

Syed, N., Martens, C.A., Hsu, W.H., 2007. Arginine vasopressin increases glutamate release and intracellular Ca^{2+} concentration in hippocampal and cortical astrocytes through two distinct receptors. J. Neurochem. 103, 229–237.

Terada, Y., Tomita, K., Nonoguchi, H., Yang, T., Marumo, F., 1993. Different localization and regulation of two types of vasopressin receptor messenger RNA in microdissected rat nephron segments using reverse transcription polymerase chain reaction. J. Clin. invest. 92, 2339–2345.

Thul, R., Bellamy, T., Roderick, H., Bootman, M., Coombes, S., 2008. Calcium oscillations. Adv. Exp. Med. Biol. 641, 1–27.

Tobin, V.A., Hashimoto, H., Wacker, D.W., Takayanagi, Y., Langnaese, K., Caquineau, C., Noack, J., Landgraf, R., Onaka, T., Leng, G., Meddle, S.L., Engelmann, M., Ludwig, M., 2010. An intrinsic vasopressin system in the olfactory bulb is involved in social recognition. Nature 464, 413–417.

Van Putten, V., Li, X., Maselli, J., Nemenoff, R.A., 1994. Regulation of smooth muscle alpha-actin promoter by vasopressin and platelet-derived growth factor in rat aortic vascular smooth muscle cells. Circ. Res. 75, 1126–1130.

Vega, J.A., del Valle-Soto, M.E., Calzada, B., Alvarez-Mendez, J.C., 1991. Immunohistochemical localization of S-100 protein subunits (alpha and beta) in dorsal root ganglia of the rat. Cell Mol. Biol. 37, 173–181.

Viero, C., Shibuya, I., Kitamura, N., Verkhratsky, A., Fujihara, H., Katoh, A., Ueta, Y., Zingg, H.H., Chvatal, A., Sykova, E., Dayanithi, G., Review: Oxytocin: Crossing the Bridge between Basic Science and Pharmacotherapy. CNS Neurosci. Ther. 16, e138–e156.

Vit, J.P., Ohara, P.T., Bhargava, A., Kelley, K., Jasmin, L., 2008. Silencing the Kir4.1 potassium channel subunit in satellite glial cells of the rat trigeminal ganglion results in pain-like behavior in the absence of nerve injury. J. Neurosci.: the official journal of the Society for Neuroscience 28, 4161–4171.

Volpi, S., Rabadan-Diehl, C., Aguilera, G., 2004. Vasopressinergic regulation of the hypothalamic pituitary adrenal axis and stress adaptation. Stress 7, 75–83.

Yibchok-Anun, S., Cheng, H., Heine, P., Hsu, W., 1999. Characterization of receptors mediating AVP- and OT-induced glucagon release from the rat pancreas. Am. J. Physiol. 277, E56–E62.